Am J Cancer Res 2016;6(5):1040-1052
www.ajcr.us /ISSN:2156-6976/ajcr0024043

Original Article

BRAF kinase inhibitor exerts anti-tumor activity against breast cancer cells via inhibition of FGFR2

Zong Xin Zhang[1], Wen Jun Jin[1], Sheng Yang[2], Cun Li Ji[2]

[1]Department of Clinical Laboratory, Huzhou Central Hospital, No. 198, Hongqi Road, Huzhou 313000, Zhejiang Province, China; [2]Department of Breast Medical Care, Huzhou Maternity and Child Health Care Hospital, Wuxing District, East Street 2, Huzhou 313000, Zhejiang Province, China

Received January 14, 2016; Accepted March 13, 2016; Epub May 1, 2016; Published May 15, 2016

Abstract: Most anti-angiogenic therapies currently being evaluated in clinical trials targetvascular endothelial growth factor (VEGF) pathway; however, the tumor vasculature can acquire resistance to VEGF-targeted therapy by shifting to other angiogenesis mechanisms. Therefore, other potential therapeutic agents that block non-VEGF angiogenic pathways need to be evaluated. Here we identified BRAF kinase inhibitor, vemurafenibas an agent with potential anti-angiogenic and anti-breast cancer activities. Vemurafenib demonstrated inhibition of endothelial cell proliferation, migration, and tube formation in response to basic fibroblast growth factor (bFGF). In ex vivo and in vivo angiogenesis assays, vemurafenib suppressed bFGF-induced microvessel sprouting of rat aortic rings and angiogenesis in vivo. To understand the underlying molecular basis, we examined the effects of vemurafenib on different molecular components in treated endothelial cell, and found that vemurafenib suppressed bFGF-triggered activation of FGFR2 and protein kinase B (AKT). Moreover, vemurafenib directly inhibited proliferation and blocked the oncogenic signaling pathways in breast cancer cell. In vivo, using xenograft models of breast cancer cells MDA-MB-231, vemurafenib showed growth-inhibitory activity associated with inhibition of tumor angiogenesis. Taken together, our results indicate that vemurafenib targets the FGFR2-mediated AKT signaling pathway in endothelial cells, leading to the suppression of tumor growth and angiogenesis.

Keywords: Vemurafenib, angiogenesis, breast cancer, FGFR2

Introduction

Breast cancer is the leading female cancer in terms of prevalence [1]. Although early stages of breast cancer can be successfully treated by surgical resection of the tumor, there is still no effective treatment for this cancer due to sustained and excessive angiogenesis [2]. Tumor growth is angiogenesis dependent, and inhibit breast cancer angiogenesis may aid the development of more effective therapeutic strategies for combating tumor [3]. Vascular endothelial growth factor receptor 2 (VEGFR2) is the major effector for execution of VEGF-stimulated cell proliferation, vascular permeability, cell migration, and cell survival, leading to angiogenesis. Given that VEGFR2 plays a predominant role in promoting angiogenesis, it's the most important target in anti-angiogenesis therapy against cancer. A number of small molecule VEGFR2 inhibitors have been reported, including sunitinib, sorafenib, and vandetanib [4]. However, other angiogenic regulatory factors switch on during cancer progression and induce resistance to existing anti-angiogenic therapy [5]. Besides VEGF, there is a family of proteins that include placenta growth factor (PlGF), acidic fibroblast growth factor (aFGF), basic fibroblast growth factor (bFGF), Fms-like tyrosine kinase 3 (Flt3), c-Met, and platelet-derived growth factor receptor-alpha (PDGFRα) directly participate in the genesis of blood capillaries and lymphatic vessels [6].

Furthermore, recent studies have identified bFGF as a direct activator of phosphatidylinositol-4, 5-bisphosphate 3-kinase (PI3K)-protein kinase B (AKT), which are key stimuli known to initiate endothelial cell migration, invasion and differentiation. AKT is a pivotal downstream tar-

get of PI3K during angiogenesis and regulates multiple cellular processes including tumor angiogenesis, cell cycle progression, cell growth, cell migration, and cell metabolism [7]. Fbroblast growth factor receptor 2 (FGFR2) activation after bFGF binding causes phosphorylation of AKY signaling resulting in increased activation of signal transducer and activator of transcription 3 (STAT3), c-Jun and nuclear factor kappa-light-chain-enhancer of activated B cells (NF-κB) p65 [8]. STAT3 is often constitutively active in many human cancer cells, including multiple myeloma, leukemia, lymphoma, and solid tumors. STAT3 is a latent transcription factor that resides in the cytoplasm. Upon activation, STAT3 dimerizes, translocates to the nucleus and binds to nuclear DNA to modulate transcription of target genes. The activation of STAT3 results in expression of many target genes including matrix metalloproteinases (MMPs), cyclooxygenase-2 (COX-2) and angiopoietin-2 (Ang-2) which are required for tumor cell migration, angiogenesis as well as metastasis [9]. Therefore, drug that inhibits bFGF-FGFR2 axis and tumor angiogenesis is a potential therapeutic strategy.

Currently, several strategies have been already reported to block the action of kinase signaling pathway besides VEGF-VEGFR2, including small molecules. Vemurafenib (PLX4032) is a novel small-molecule BRAF inhibitor, which was approved by the Food and Drug Administration for the treatment of patients with melanoma [10]. BRAF is a major component of the RAS/RAF/MEK/MAPK signaling pathway that functions to transmit extracellular signals from the cytoplasmic membrane to the nucleus. Crosstalk between this pathway and other important cellular signaling cascades, such as PI3K/AKT/mammalian target of rapamycin (mTOR), has been the focus of extensive research and had led to a detailed understanding of BRAF's role in cellular proliferation, differentiation, migration, and angiogenesis [11]. Meanwhile, extracellular regulated protein kinases 1/2 (ERK1/2) phosphorylation, pro-angiogenic VEGF-A mRNA and total VEGF-A protein expression are decreased by vemurafenib treatment in melanoma cells [12], which indicates vemurafenib decrease the gene expression of certain mediators of angiogenesis. In addition, vemurafenib therapy significantly reduces secreted VEGFA, VEGFC and interleukin-6 (IL-6) protein levels in thyroid carcinoma cells. As a result, the secretome from vemurafenib-treated thyroid carcinoma cells inhibits micro-vascular endothelial cell-related in vitro angiogenesis [13]. Therefore, those studies provide part of molecular mechanisms for how vemurafenib contributes to anti-angiogenesis. However, data on the influence of vemurafenib on breast cancer angiogenesis and the underlying mechanisms are yet to be fully elucidated. In the present study, we investigate the effects of BRAF inhibitor, vemurafenib on angiogenesis and the growth of human breast cancer cells in vitro and in nude mouse xenograft. The results obtained provide evidence for the broader use of vemurafenib as an anti-angiogenesis agent against human breast cancer.

Materials and methods

Cell culture and plasmids

Human breast cancer lines (MCF-7, MDA-MB-231, T-47D, Bcap-37) and SV40-immortalized non-tumorigenic human bronchial epithelial cells BEAS-2B were obtained from the Chinese Academy of Sciences Cell Bank of Type Culture Collection (CBTCCCAS, China), and maintained in DMEM or RPMI-1640 medium supplemented with 10% FBS. Human umbilical vein endothelial cells (HUVEC) was purchased from Chi Scientific, and were cultivated in gelatinized culture plates in M199 medium supplemented with 15% FBS and 50 mg/ml endothelial cell growth supplement (ECGS, BD Bioscience). Hemagglutinin (HA)-tagged constitutively active mutant D2AKT (T308D/S473D-AKT) plasmid was deposited by Takashi Tsuruo [14]. Transfection was performed with lipofectamine 2000 following the manufacture's manual. Vemurafenib (Selleck, S1267) was dissolved in dimethyl sulfoxide (DMSO, final concentration is 0.1%) to prepare required concentrations.

Cell proliferation assay

The cell viability was determined by CellTiter 96® Aqueous One Solution cell proliferation assay (Promega). Briefly, cells were seeded in 96-well cell culture plates and treated with indicated agents. After incubation for indicated time period, 20 ml of One Solution reagent were added to each well and incubation was

continued for additional 4 h. The absorbance was measured at 490 nm using Synergy™ HT Multi-Mode Microplate Reader. The effect of indicated agents on cell viability was assessed as the percent of cell viability compared with vehicle-treated control cells, which were arbitrarily assigned 100% viability [15]. The concentration of vemurafenib resulting in 50% inhibition of control growth (IC50) was calculated.

Wound healing assay

We examined the migration of HUVEC using a wound-healing assay. Briefly, cells were each grown on 3.5-cm plates with their respective culture media. After the growing cell layers had reached confluence, we inflicted a uniform wound in each plate using a pipette tip, and washed the wounded layers with PBS to remove all cell debris. Then, we evaluated the closure at 48 h using bright-field microscopy.

Invasion assay

Assay was performed with Matrigel-coated chambers from a BioCoat Matrigel Invasion Chamber Kit (BD Biosciences). Cells with 500 μl in serum-free medium were added into the upper chamber and complete medium was added into the lower chamber. After incubation for 24 h, non-invasive cells in the upper surface of the membrane were removed and the cells invasion to the lower surface of the membrane was fixed. Cell counting was then carried out by photographing the membrane through the microscope and five random fields were taken.

Tube formation assay

Assay was performed using 12-well plate coated with 100 ml Matrigel basement membrane matrix (BD Bioscience) per well and polymerized at 37°C for 30 min. HUVEC suspended in M199 medium containing 2% FBS were plated on the Matrigel at a density of 2×10^5 cells/well. Vemurafenib were then added together with bFGF. After 8 h, The Matrigel-induced morphological changes were photographed and the extent of capillary tube formation was evaluated by measuring the total tube length per field.

Rat aortic ring assay

In brief, 48-well plates were coated with 120 μl of Matrigel per well and polymerized in an incubator. Aortas isolated from 6-week-old male Sprague-Dawley rats were cleaned of periadventitial fat and connective tissues in cold phosphate-buffered saline and cut into rings of 1~1.5 mm in circumference [16]. The aortic rings were randomized into wells and sealed with a 100 ml overlay of Matrigel. bFGF in 500 ml of serum-free M199 with or without vemurafenib was added into the wells, and the fresh medium was exchanged for every 2 d. After 6 d, micro-vessel sprouting was photographed using an inverted microscope (Olympus).

Chick chorioallantoic membrane assay

Chick chorioallantoic membrane (CAM) assay was performed, as described previously [17].

Matrigel plug assay

All animal care and experimental procedures were compliant with the guidelines of Institute for Experimental Animals, Department of Clinical Laboratory, Huzhou Central Hospital and approval to conduct the animal experiments had been obtained from this committee. The Matrigel plug assay in BALB/c mice was performed as described previously [18]. Prepared Matrigel was then injected subcutaneously into the flanks of 6-week-old BALB/c male mice. After 7 days, the Matrigel plugs were removed and the hemoglobin content of the Matrigel plugs was quantified using QuantiChrom™ Hemoglobin Assay Kit (BioAssay Systems).

Anchorage-independent cell growth in soft agar

MDA-MB-231 cells (5×10^4) suspended in 2 ml medium, 0.3% agar, and 10% FBS were plated over the bottom agar pre-solidified with 3 ml medium containing 0.6% agar and 10% FBS. Colony formation was then carried out by photographing through the microscope after 14 days. Five random fields under microscope were taken and colony formation unities were counted.

FGFR2 kinase inhibition assay

The IC50 value for inhibition of FGFR2 by vemurafenib was determined using a FGFR2 Kinase Assay/Inhibitor Screening Kit (KA0057, Abnova)

according to the manufacturer's instructions [19].

Western blot analysis

Whole-cell lysates were prepared with RIPA buffer containing protease and phosphatase inhibitors. Equal amounts of cell lysates (25 μg) were loaded on 10% SDS-PAGE and transferred onto PVDF membranes. After membranes were blocked, they were incubated with monoclonal antibody against phosphorylation/total FGFR2, PI3Kp85, AKT, STAT3, ERK1/2, MMP-2/9, and GPADH (CST) followed by incubation with horseradish peroxidase-conjugated IgGs. Target proteins were detected by the ECL system (Millipore) and visualized with the ChemiDoc XRS system (Bio-Rad).

Immunoprecipitation assay

HUVEC were lysed in a culture dish by adding 0.5 mL of ice-cold RIPA lysis buffer. The supernatants were collected and then incubated with IgG or bFGF in presence or absence of vemurafenib at 4°C overnight, followed by incubation with anti-FGFR2. Then, supernatants were incubation with protein G-Sepharose (Santa Cruz). Following the removal of supernatant by brief centrifugation, the protein G-Sepharose were washed with lysis buffer and then boiled for 10 minutes in loading buffer. Immunoprecipitates was further analyzed by western blotting using anti-FGFR2antibody and anti-bFGF antibody.

Matrix metalloproteins (MMPs) activity assay

The activity of MMP-2/9 was determined by QuickZyme MMPs activity assay (QucikZymeBioSciences) according to the manufacturer's instructions [20].

Immunocytochemistry

HUVEC were fixed with 4% paraformaldehyde for 30 min, permeabilized with 0.1% Triton X, and blocked with 3% BSA for 30 min. Subsequently, the cells were immune-stained by incubating with antibody against p-AKT^{Thr308} overnight at 4°C. After being washed with PBS, cells were incubated with FITC-conjugated goat anti-rabbit secondary antibody (Boster Biotechnology). Nuclei were stained with 4', 6-diamino-2-phenylindole (DAPI; Invitrogen).

Subcutaneous xenograft models

MDA-MB-231 cells (3×10^6) were subcutaneously implanted into female, BALB/c nude mice to build non-small cell lung cancer xenograft. Tumor volume and mice body weight were measured every 3 days [20]. Tumor volume was calculated as $mm^3 = 0.5 \times \text{length } (mm)^3 \text{ width } (mm)^2$. After sacrificing mice on day 25, tumors tissues will be harvested for western blotting. Deparaffinized tumor sections were stained with specific antibodies including Ki67, p-FGFR-2^{Tyr463}, p-PI3K p85^{Tyr458}, p-AKT^{Thr308}, and anti-CD31 FITC antibody. Detection was done with avidin-biotin-HRP complex (Thermo scientific) and diaminobenzidine as chromogen. Nuclei were counterstained with hematoxylin. All animal experiments were carried out in compliance with the Guidelines for the Institute for Experimental Animals, Department of Clinical Laboratory, Huzhou Central Hospital.

Statistical analysis

The data were presented as mean ± SD. Differences in the results of two groups were evaluated using either two-tailed Student's t test or one-way ANOVA followed by post-hoc Dunnett's test. The differences with $P < 0.05$ were considered statistically significant.

Results

Tumor angiogenesis associated kinases inhibition profile of vemurafenib

Angiogenesis a complex process by which new blood vessels are formed via proliferation of vascular endothelial cells. A variety of pro-angiogenesis factors including vascular endothelial growth factor (VEGF) and basic fibroblast growth factor (bFGF) have recently been identified. In this study, vemurafenib was screened by kinase inhibition assay by the use of radiometric assays provided by Kinase Profile Service (Millipore, UK). As shown in **Table 1**, vemurafenib exhibited great inhibitory activity on FGFR2 with an inhibitory rate of 85% at 100 nM. In addition, vemurafenib showed a relatively low inhibitory rate of 24%, 4%, 1%, and 2% against FGFR1, VEGFR2, PDGFR-α, and PDGFR-β at 100 nM, respectively. Moreover, excellent selectivity for FGFR2 was evident compared with a range of unrelated tyrosine and serine/threonine kinases, including Flt3,

Table 1. In vitro profile of vemurafenib against a panel of 20 kinases. The assays were performed in three independent experiments. Data are means ± SD

Kinase	Inhibition rate at 100 nM (%)
FGFR1	24 ± 3
FGFR2	85 ± 1
VEGFR2	4 ± 0
Flt3	8 ± 2
PDGFR-α	1 ± 0
PDGFR-β	2 ± 0
c-Kit	6 ± 1
Aurora-A	-2 ± 2
Haspin	7 ± 2
ErbB4	10 ± 2
IKKβ	-5 ± 2
c-Met	11 ± 0
CDK2	-13 ± 2
PI3K	20 ± 1
EGFR	4 ± 1
JNK	-9 ± 0
mTOR	5 ± 2
GSK3β	4 ± 0
KRAS	18 ± 4
JAK	5 ± 1

c-Kit, c-Met, epidermal growth factor receptor (EGFR), KRAS etc.

Vemurafen inhibits endothelial cells growth

We initially sought to evaluate the inhibitory activity of vemurafenib on endothelial cell proliferation, and to evaluate the specificity of this effect for distinct angiogenic stimuli, including VEGFA, aFGF, bFGF, platelet-derived growth factor (PDGF), IL-8, or phosphatidylinositol-glycan biosynthesis class f protein (PIGF). The proliferation of HUVEC stimulated by bFGF rather than other angiogenic stimuli was markedly decreased after vemurafenib treatment ranging from 10 nM to 50 nM (**Figure 1A**). To determine the concentration of vemurafenib that does not induce cytotoxicity in HUVEC in the absence of bFGF, HUVEC cells were initially treated with vemurafenib (5-70 nM) for 24 h, and the cell viability was evaluated by MTT assay. As shown in Figure S1, vemurafenib did not significantly affect cell viability up to 40nM, but over 50 nM vemurafenib exhibited a cytotoxic effect in HUVEC compared to control. To validate whether vemurafenib would result in toxicity effects on HUVEC, LDH cytotoxicity assay was carried out. As shown in Figure S2, Triton X-100 markedly increased LDH release and vemurafenib brought little toxic effects on HUVEC when compared to vehicle control. Therefore, further analyses of the biological activities of vemurafenib were performed using less than a 40 nM concentration of vemurafenib in endothelial cells.

Since angiogenic stimuli stimulate cellular responses by binding to tyrosine kinase receptors on the cell surface, causing them to dimerize and become activated through trans-phosphorylation, we examined whether vemurafenib exposure altered the activity state of FGFR2. Analysis of phospho-tyrosine level on FGFR2 in HUVEC cultured in bFGF revealed vemurafenib decreased the phosphorylated FGFR2 level in a dose-dependent manner (**Figure 1B**). To investigate whether vemurafenib decreased the kinase activity of FGFR2, we performed in vitro kinase assay with different concentrations of vemurafenib using FGFR2 Kinase Assay Kit (Abnova) according to manufacturer suggested method. Our data demonstrated that vemurafenib directly inhibited FGFR2 kinase activity in a dose-dependent manner with an IC50 of ~39.95 nM (**Figure 1C**). All these results indicated that vemurafenib was a potent FGFR2 inhibitor. Strikingly, immunoprecipitation-western blot analysis using HUVEC revealed that vemurafenib did not affect bFGF binding to FGFR2, which suggesting vemurafenib was an irreversibly FGFR2 inhibitor (**Figure 1D**).

Vemurafenib inhibits bFGF induced HUVEC migration and invasion

Endothelial cell migration and invasion are essential processes in angiogenesis. We explored the effects of vemurafenib on bFGF stimulated endothelial cell migration and invasion using wound-healing and Transwell invasion assay. We found that vemurafenib inhibited bFGF-stimulated HUVEC motility in a dose-dependent manner (**Figure 2A**). Vemurafenib also markedly inhibited invasion of HUVEC under stimulation with bFGF (**Figure 2B**). Taking into account that matrix metalloproteinases (MMPs) such as MMP-2 and MMP-9 are involved in the development of several human malignancies, as degradation of collagen IV in

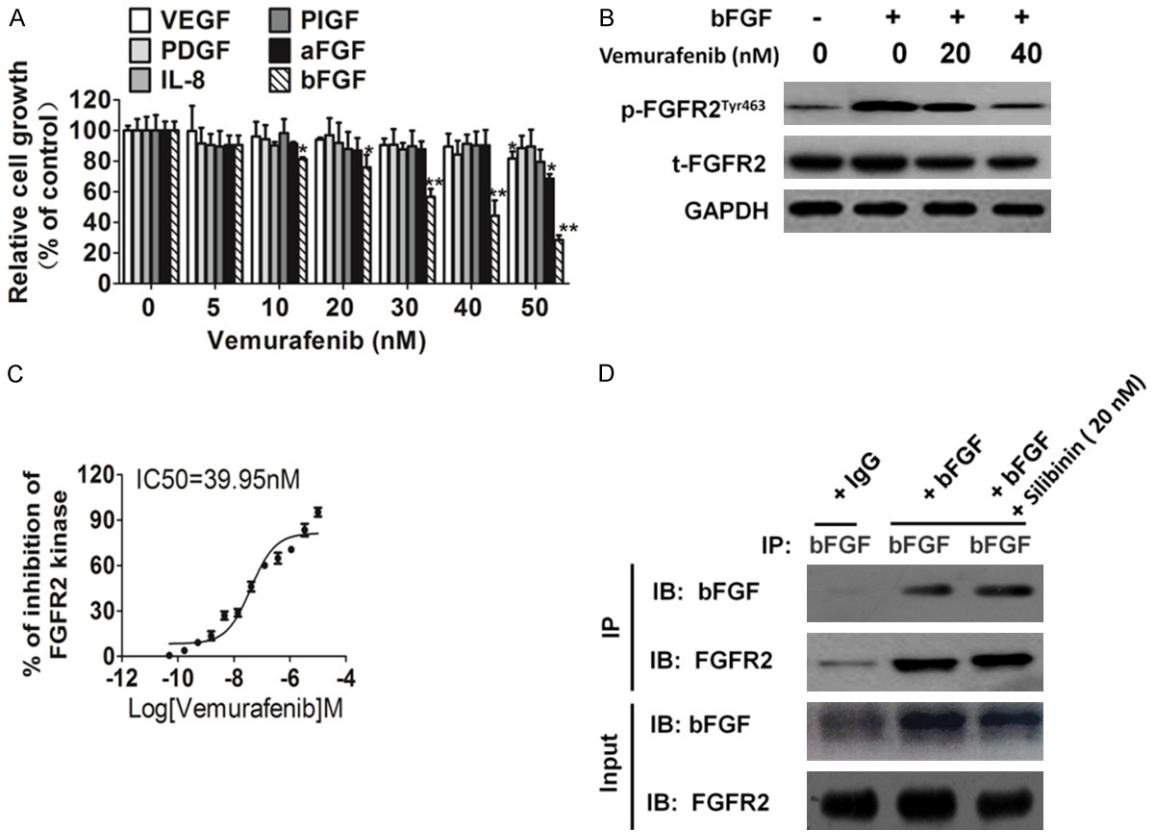

Figure 1. In vitro treatment of HUVEC with vemurafenib inhibited the proliferation. A. Vemurafenib markedly inhibited HUVEC proliferation in a dose dependent manner in cultures stimulated by supplementation with bFGF. B. Inhibition of bFGF-induced FGFR2 tyrosine phosphorylation by vemurafenib. C. Vemurafenib exhibited great inhibitory activity on FGFR2 with an inhibitory rate of 50% at 39.95 nM. D. Immunoprecipitation-western blot assay to analyze the binding of bFGF with the FGFR2 in the presence of vemurafenib. Data are from three independent experiments and are mean ± SD.

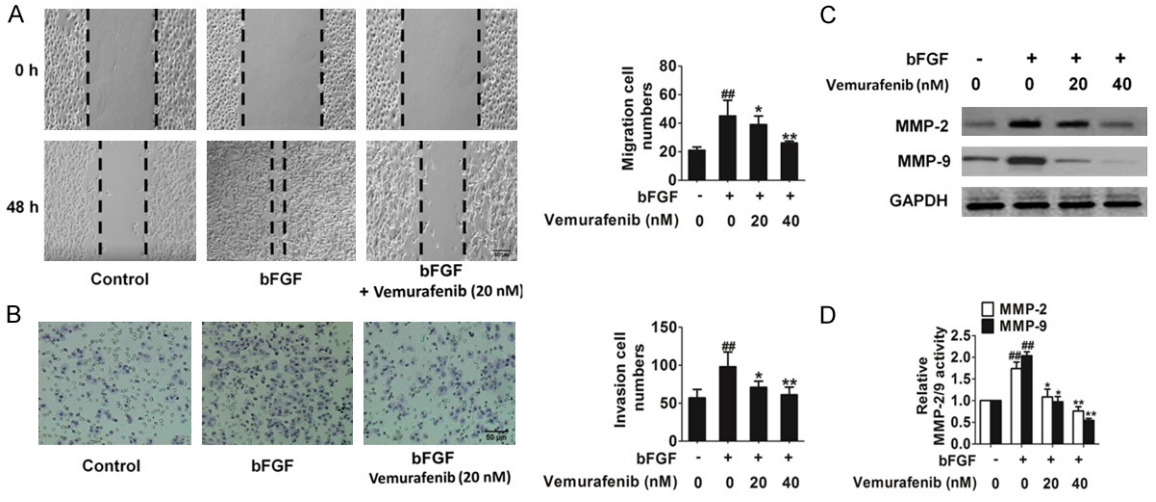

Figure 2. Vemurafenib inhibited HUVEC mobility in vitro. A. Vemurafenib remarkably inhibited bFGF-induced HUVEC migration measured by wound healing assay. Scale bar represents 50 μm. B. Vemurafenib strongly suppressed bFGF-induced HUVEC invasion measured by Transwellassay. Each experiment was performed in duplicate. All data were expressed as mean ± SD. $^{\#\#}P < 0.01$ versus control, $^{*}P < 0.05$; $^{**}P < 0.01$ versus bFGF alone. Scale bar represents 50 μm. C. Biochemical analysis of MMP-2/9 in HUVEC cells undervemurafenib treatment. Protein loading was

normalized by GAPDH. D. Quantification of MMP-2/9 activity in HUVEC treatment with vemurafenib in the presence of bFGF. Data are from three independent experiments and are mean ± SD. $^{\#\#}P < 0.01$ compared with control, $^{*}P < 0.05$, $^{**}P < 0.01$ compared with bFGF alone treatment.

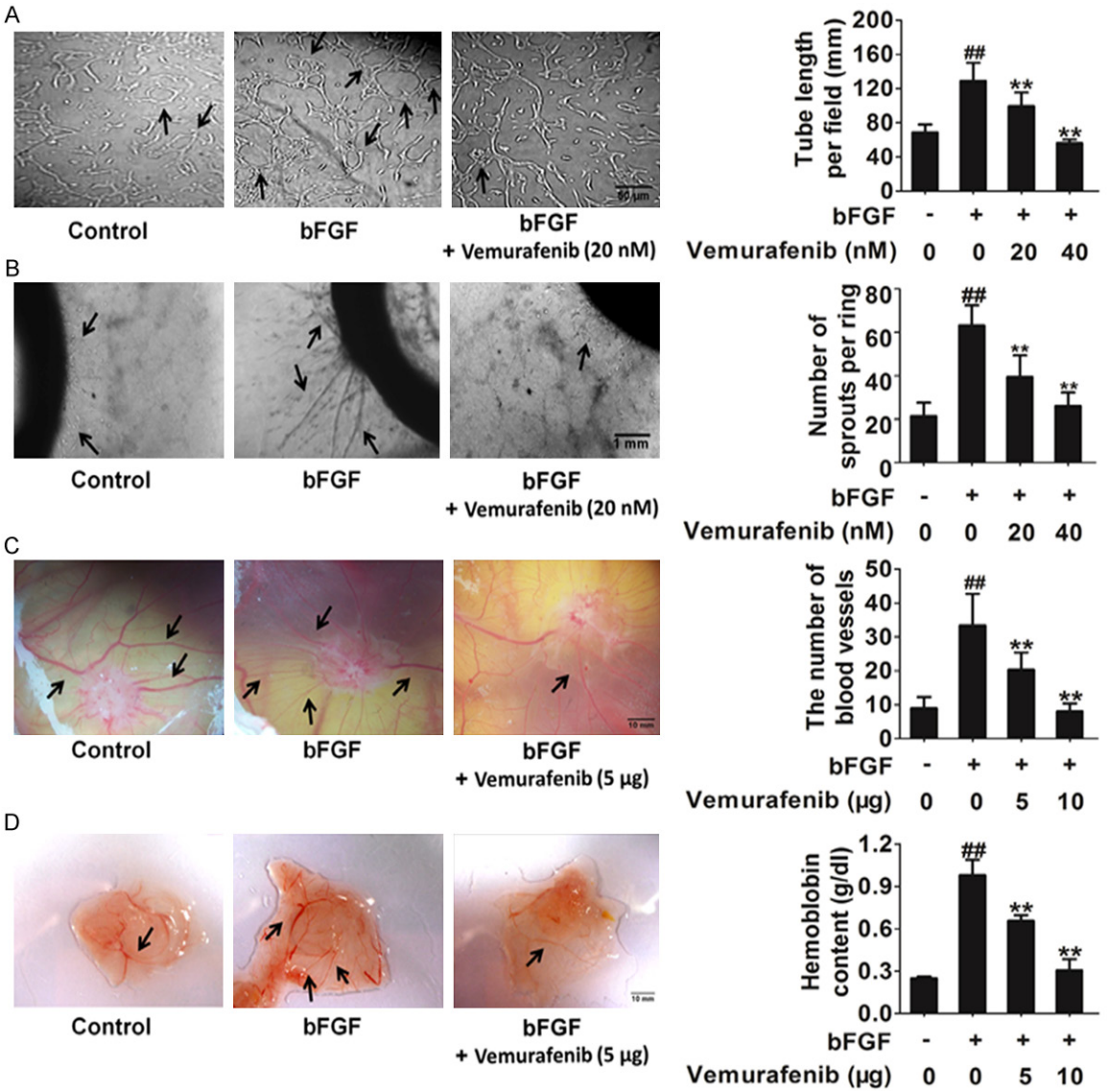

Figure 3. Vemurafenib inhibited bFGF-induced angiogenesis. A. Vemurafenib inhibited HUVEC tube formation. HUVEC were seeded on Matrigel layer and treated with bFGF in the presence or absence of vemurafenib. Scale bar represents 50 μm. B. Vemurafenib dose dependently suppressed sprout formation on the organotypic model of rat aortic ring. Scale bar represents 1 mm. C. CAM assay. Photopictographs of a typical experiment showing the angiogenesis pattern in different treatments.Scale bar represents 10 mm. D. Matrigel mixed with bFGF or vemurafenib was injected into the flanks of BALB/c mice. Seven days later, the Matrigel plugs were removed for analysis. Representative appearance of Matrigel plugs. Hemoglobin content of Matrigel plugs from groups of mice was quantified by using QuantiChrom™ Hemoglobin Assay Kit. Each experiment was performed in duplicate. Scale bar represents 10 mm. All data were expressed as mean ± SD. $^{\#\#}P < 0.01$ versus control, $^{*}P < 0.05$; $^{**}P < 0.01$ versus bFGF alone.

basement membrane and extracellular matrix facilitates tumor progression, including metastasis and angiogenesis, we analyzed their levels and activity. A significant drop in MMP-2/-9 expression levels were observed in vemurafenib treated HUVEC (**Figure 2C**). Quantification of MMP-2/-9 activities using a fluorogenic assay showed a significantly decrease in extracellular MMP-2/-9 activity in HUVEC treated with vemurafenib (**Figure 2D**).

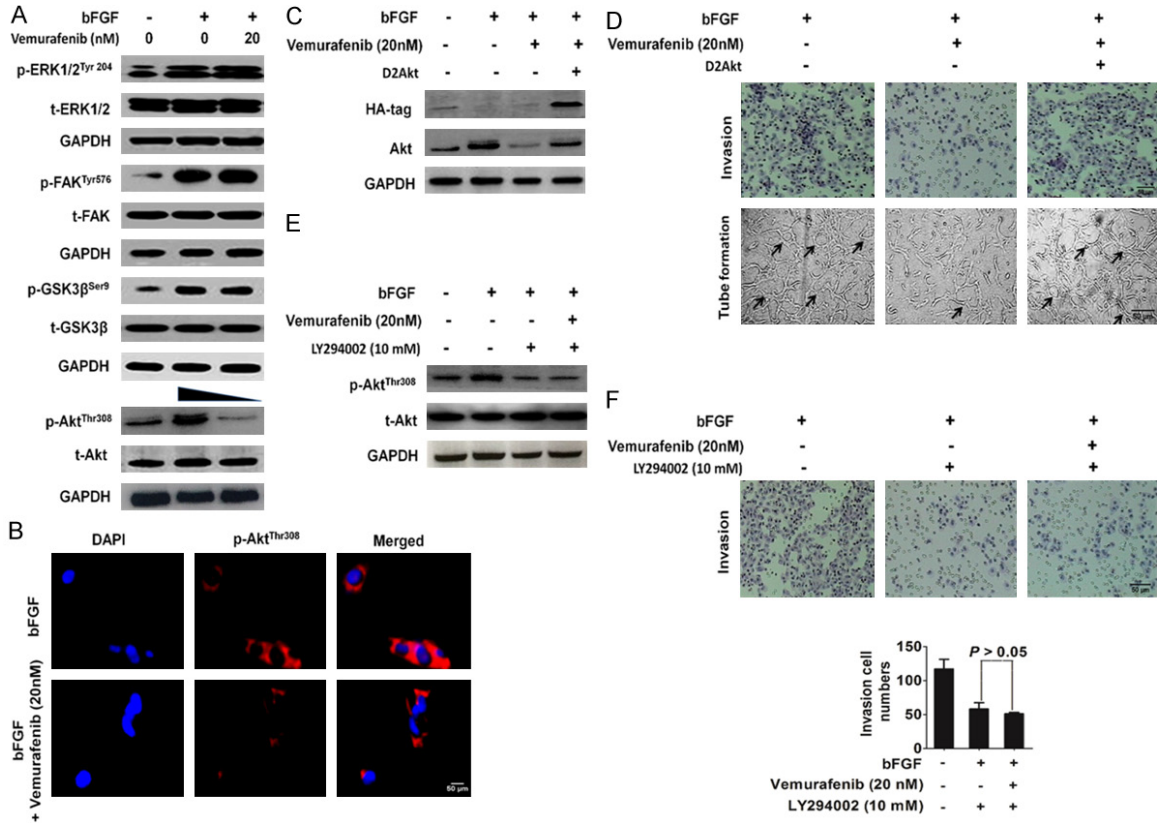

Figure 4. Vemurafenib inhibited invasion and tube formation of HUVEC via Akt pathway. A. Western blot shown that the phosphorylation of Akt at Thr308 was inhibited in cells treated with vemurafenib. B. Vemurafenib reducedphosphorylated Akt in HUVEC. Cells were treated with vemurafenib for 4 h and processed for immunofluorescence staining with antibodies against p-Akt^{Thr308}. Cell nuclei were stained with DAPI. Scale bar represents 50 μm. C. Constitutively active form of Akt (D2Akt) was introduced into cells and expression of D2Akt was confirmed by western blot, and GAPDH was used as loading control. D. Transwell assayand tube formation assay were performed to determine vemurafenib inhibit HUVEC angiogenesis process dependent on inactivation of Akt. Scale bar represents 50 μm. E. In the presence of LY294002, protein extracts were analyzed by western blot with antibody against phosphorylated Akt (Thr308) or Akt. F. Transwell assay was conducted to evaluate the cell invasiveness in the presence of LY294002. Representative pictures were taken after staining with crystal violet. Scale bar represents 50 μm. Each experiment was performed in duplicate. All data were expressed as mean ± SD. $P > 0.05$, vemurafenib combined with LY294002 versus LY294002 alone treated group.

Vemurafenib potently inhibits bFGF-induced microvessel sprouting ex vivo and angiogenesis in vivo

Beyond endothelial cell proliferation and migration, neovascularization is dependent on angiogenic stimuli driving formation and organization of tubular networks. We utilized this tube formation analysis to further define dose-dependent effects of vemurafenib in response to bFGF stimuli. In this assay, vemurafenib inhibited tube network formation in a dose-dependent manner (**Figure 3A**). To future evaluate the potential effect of vemurafenib on angiogenesis, three well-established angiogenesis models were used ex vivo and in vivo. We determined the effects of vemurafenib on micro-vessel sprouting ex vivo using the rat aortic ring assay. Our results showed that vemurafenib almost completely inhibited bFGF-induced sprouting from the aortic rings (**Figure 3B**). Furthermore, in the CAM assay, bFGF could significantly induce neovascularization, whereas treatment with 5 μg/CAM of vemurafenib potently inhibited bFGF-induced neovascularization (**Figure 3C**). Matrigel plug assay had also been used to evaluate the effects of vemurafenib on bFGF-induced angiogenesis in vivo. As shown in **Figure 3D**, Matrigel plugs containing bFGF was filled with intact red blood cells, indicating that functional vasculatures had formed inside the Matrigel via angiogenesis

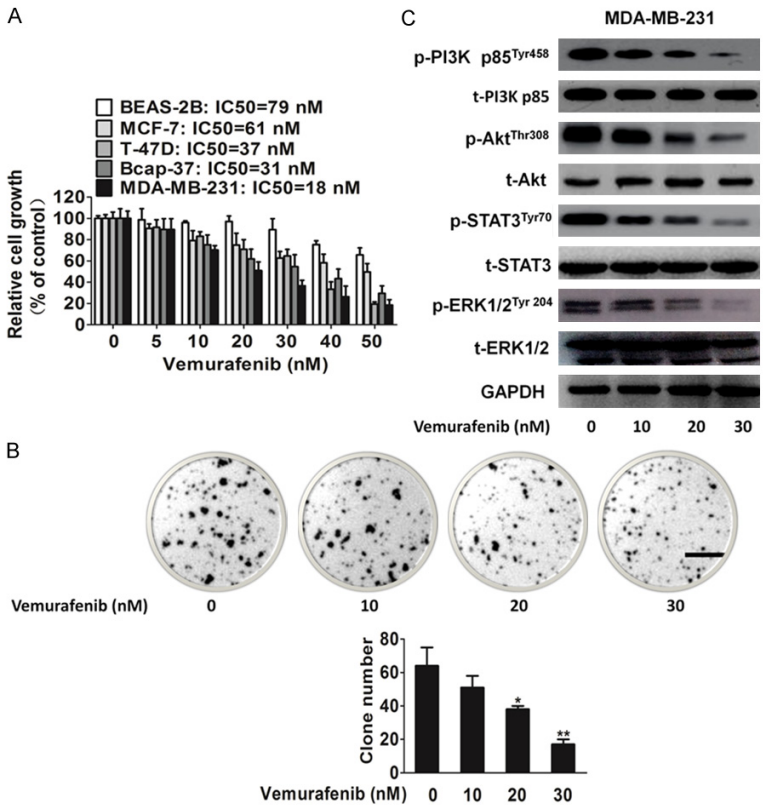

Figure 5. Inhibitory effects of vemurafenib on tumor cells. A. Vemurafenib inhibited cell viability in breast cancer cells. The concentration of vemurafenib resulting in 50% inhibition of control growth (IC50) was calculated. B. Vemurafenibinhibited anchorage-independent growth of MDA-MB-231 cells. Scale bar represents 1 mm. C. Vemurafenib inhibited oncogenic signaling pathways in MDA-MB-321 in vitro. All data were expressed as mean ± SD. $^{**}P < 0.01$ versus vehicle.

triggered by bFGF. In contrast, addition of vemurafenib dramatically inhibited vascular formation. Ten hemoglobin content in the Matrigel plugs showed that vemurafenib at a dose of 5 μg dramatically blocked bFGF-induced vasculature formation in vivo.

AKT pathway involves in anti-angiogenesis activity of vemurafenib

To determine the signaling pathways which were correlated with vemurafenib-inhibited HUVEC migration and tube formation, multiple potential signaling pathways were screened in the present study. As shown in **Figure 4A** and **4B**, only the basal level of AKT activation was found to be significantly down-regulated. In contrast, no obvious difference could be observed for many other signaling pathways, such as FAK, ERK and glycogen synthesis kinase 3β (GSK-3β). To confirm the role of AKT in the inhibition of vemurafenib on migration and tube formation, constitutively active form of AKT (D2AKT) was introduced into HUVEC and the expression of D2AKT was confirmed by western blot with anti-HA-tag and anti-AKT antibody (**Figure 4C**). As expected, active AKT restored HUVEC migration and tube formation (**Figure 4D**). As expected, the biological behavior of endothelial cells was not inhibited by vemurafenib in the presence of D2AKT. In view of the AKT signaling pathway potential involve in the inhibition effect of vemurafenib on angiogenesis, and together with the above observations, it could be postulated that inhibition of AKT activation might deter the anti-angiogenesis effect of vemurafenib. To this end, we observed that there were no difference between vemurafenib treatment and vemurafenib plus AKT inhibitor LY294002 as illustrated in western blot (**Figure 4E**) and Transwell assay (**Figure 4F**). To conclude, these data indicate that AKT signaling is involved in vemurafenib inhibit angiogenesis of HUVEC.

Vemurafenib inhibits breast cancer cells growth

To assess the inhibitory activity of vemurafenib on breast tumor cell growth, the anti-proliferative effects of vemurafenib were examined in a panel of breast cancer cell lines. In these cell lines, vemurafenib had appreciable effect on proliferation, especially in MDA-MB-231 (**Figure 5A**). To verify whether vemurafenib could inhibit anchorage-independent growth of MDA-MB-231 cells, we performed soft agar colony formation assay. Vemurafenib greatly decreased, in a dose-dependent manner, the number and the size of colonies of MDA-MB-231 cells grown (**Figure 5B**). To gain further insight into the molecular mechanism of the inhibitory effects of vemurafenib on tumor cells, we evaluated the expression of PI3K, AKT, STAT3, and ERK1/2 in MDA-MB-231 cells.

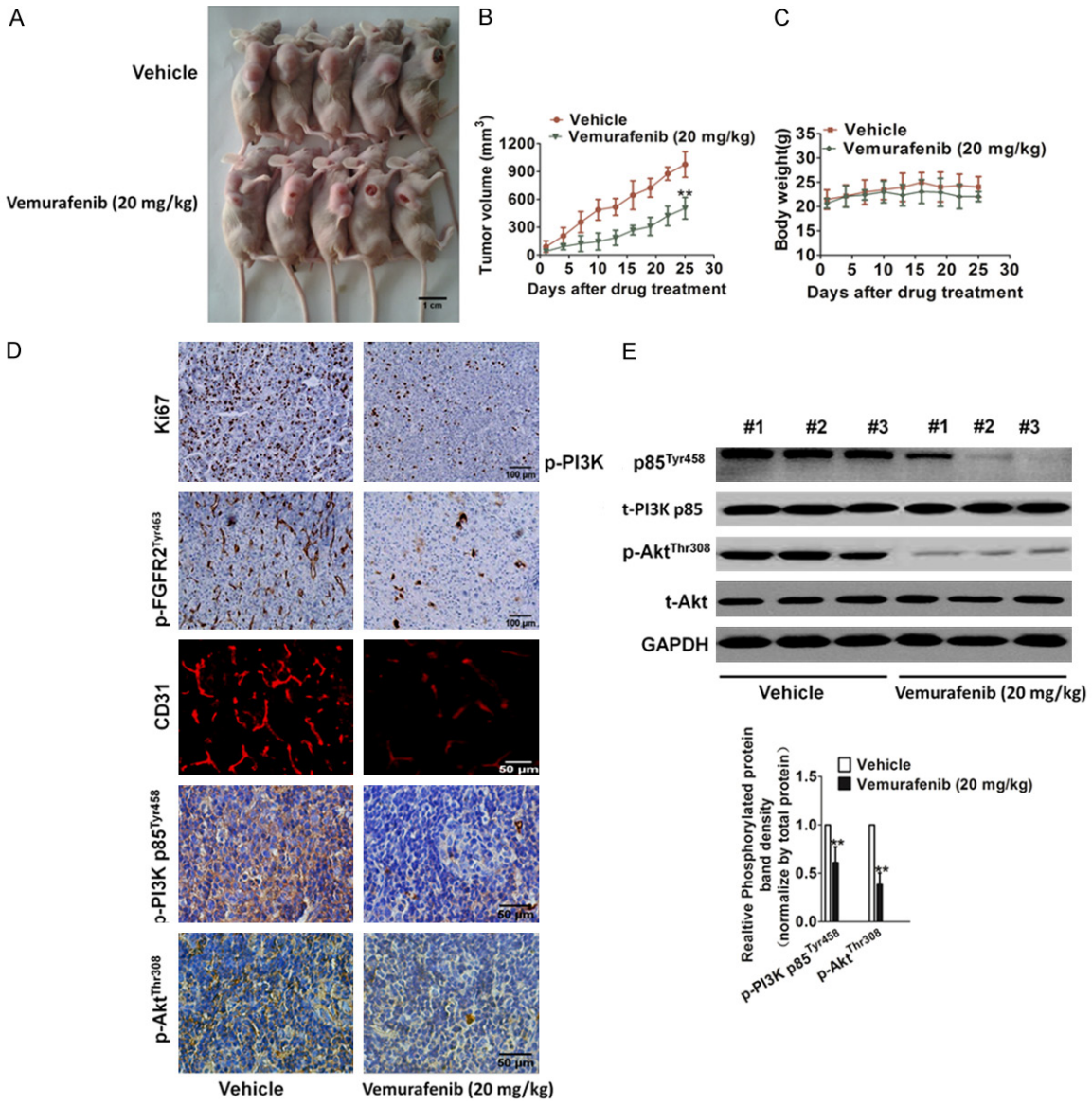

Figure 6. Inhibitory effects of vemurafenib on tumor growth and angiogenesis. A. Vemurafenib inhibited tumor growth in xenograft mice. MDA-MB-231 cells were injected into nude mice and the mice were treated with or without vemurafenib at a dosage of 20 mg/kg daily. Scale bar represents 1 cm. B. Vemurafenib inhibited tumor volume. All data were expressed as mean ± SD. $^{**}P < 0.01$ versus vehicle. C. Vemurafenib had no toxic effect on mouse body weight. All data were expressed as mean ± SD. D. Vemurafenib suppressed tumor angiogenesis. The tumor tissues were immunohistochemistry analysis using anti-Ki67, anti-p-FGFR2^{Tyr463}, anti-CD31 FITC, anti-p-PI3K, and anti-p-AKT antibodies. E. Vemurafenib suppressed p-PI3K and p-AKT expression in solid tumors. # represents mice number. Each experiment was performed in duplicate.

As shown in **Figure 5C**, vemurafenib dramatically decreased the expression of phosphorylated PI3K, AKT, STAT3, and ERK1/2, whereas the total protein levels were not significantly changed.

Vemurafenib inhibits tumor growth and angiogenesis in a xenograft mouse model

To investigate the effect of vemurafenib on tumor growth and tumor angiogenesis in vivo, we applied vemurafenib in a breast cancer cell (MDA-MB-231) xenograft model. We found that administration of 20 mg/kg/d vemurafenib for 25 d substantially suppressed tumor volume (**Figure 6A** and **6B**). However, vemurafenib had no significant effect on the body weight of mice (**Figure 6C**), suggesting low toxicity of vemurafenib at the test dosage and conditions. We observed significant reduction in Ki67 staining in the vemurafenib treatment group, indicating

a decrease in proliferating cells in tumor tissues as shown in **Figure 6D**. Furthermore, tumor sections stained with anti-p-FGFR2^{Tyr463} and anti-CD31 FITC antibody revealed that vemurafenib inhibited angiogenesis in vivo (**Figure 6D**). In addition, vemurafenib treatment also resulted in down-regulation of PI3K-AKT signaling. As shown in **Figure 6E**, vemurafenib also decreased phosphorylation of PI3K and AKT in MDA-MB-231 xenograft tumors, which was consistent with the results of MDA-MB-231 cells in vitro. The data indicated that vemurafenib could inhibit angiogenesis in vivo, which contributes to tumor growth suppression.

Dissuasion

Breast cancer remains one of the most common cancers as well as one of the leading causes of worldwide cancer-related morbidity and mortality. Conventional treatment for breast cancer includes surgery, radiation, and chemotherapy. Despite the fact that these treatment modalities have improved over the last decade, the prognosis of this cancer patients remains poor [21]. Cancer-associated angiogenesis is a critical component of solid tumor establishment, growth, and spread, and remains a primary target of anti-cancer drug development. Anti-angiogenic agents prolong the survival of cancer patients, however, without cure and at the expense of side effects. The role of VEGF and VEGFR-2 in tumor growth is well established, but other angiogenic factors switch on during cancer progression and induce resistance to VEGFR inhibitors. As such, novel compounds that could be more effective with potentially less side effects are critically needed.

bFGF is a pleiotropic cytokine that stimulates endothelial cell growth, migration, and survival. FGFR2 is one of four FGFR genes that encode a complex family of transmembrane receptor tyrosine kinases. FGFR2 is composed of three immunoglobulin (Ig)-like extracellular domains, two of which are involved in ligand binding, a single transmembrane domain, a split tyrosine kinase, and a C-terminal tail with multiple autophosphorylation sites. Unlike VEGF, bFGF selectively binds its receptor FGFR2 and stimulates angiogenesis, tumor growth and endothelial cell migration, indicating that bFGF has biological activity in vivo [22]. FGFR2 is a key regulator of tumor development which plays vital roles in regulating tumor cell proliferation, differentiation and angiogenesis. Previous studies have demonstrated that FGFR2 promotes angiogenesis and tumor growth through the PI3K/AKT downstream pathway [23].

Our group has been engaged in the screening of novel angiogenesis inhibitors and in the present study, we examined a small novel molecule vemurafenib as a potent tumor angiogenesis inhibitor. Vemurafenib has been shown to cause programmed cell death in melanoma cell lines by interrupting the B-Raf/MEK/ERK pathway. In assays of endothelial cell proliferation, vemurafenib consistently demonstrated potent anti-proliferative activity in cultures stimulated with bFGF. Beyond proliferation, endothelial cell migration, invasion, and complex tube formation are all critical, and distinct, functional components of tumor-associated angiogenesis. Vemurafenib potently inhibited each of these functional competencies as indicated by our results in vitro assays. Supporting evidences concerning anti-angiogenesis effects of vemurafenib then come from obviously inhibited sprouts formation in rat aortic ring assay. Notably, we also found that vemurafenib pose significant inhibition to angiogenesis in vivo based on CAM and Matrigel plug assay. Probing of phosphorylation and activation status of FGFR2 revealed that vemurafenib has the capacity to inhibit activation of FGFR2, which is a critical receptor primarily responsible for angiogenic response to bFGF. Activation of AKT is necessary for angiogenesis and regulates several endothelial cell functions such as migration and proliferation [24]. In this study, the underlying molecular mechanism for vemurafenib inhibits angiogenesis is identified to be related to AKT signaling pathway. Our results showed that restored AKT activity by an active form AKT plasmid could rescue the impaired migration and tube formation of endothelial cell inhibited by vemurafenib. In the presence of AKT inhibitor, vemurafenib could no longer inhibit AKT activity and invasion of endothelial cell.

Besides inhibiting tumor angiogenesis, vemurafenib also had a direct inhibitory effect on tumor cells. Vemurafenib inhibited the proliferation of breast cancer cells, which is most sensitive to MDA-MB-231 vemurafenib treatment among the cancer cells treated. Extending

these analyses in vivo, vemurafenib obviously inhibited tumor growth inhuman melanoma xenograft model. Histological studies of tumor sections revealed that vemurafenib significantly reduced angiogenesis indexed by CD31 and p-FGFR2^{Tyr463} antibodies. Meanwhile, western blot and immunohistochemistry results show that vemurafenib treatment could attenuate expressions of p-PI3K and p-AKT, further demonstrating that vemurafenib played an important role in suppressing angiogenesis at least in part via FGFR2 signaling pathway. In conclusion, our data clearly demonstrate that vemurafenib exerts a potent anti-angiogenic, and anti-tumor growth effects on breast cancer by targeting FGFR2 signaling pathway. Our findings provide the first instance of the potential role of vemurafenib as an anti-breast cancer agent, and certainly deserve more attention for further explorations to identify novel effective therapeutic compounds against breast cancer.

Disclosure of conflict of interest

None.

Address correspondence to: Cun Li Ji, Department of Breast Medical Care, Huzhou Maternity and Child Health Care Hospital, Wuxing District, East Street 2, Huzhou 313000, Zhejiang Province, China. E-mail: jicunli0898@sina.com

References

[1] Rossi RE, Pericleous M, Mandair D, Whyand T, Caplin ME. The role of dietary factors in prevention and progression of breast cancer. Anticancer Res 2014; 34: 6861-75.

[2] Yadav L, Puri N, Rastogi V, Satpute P, Sharma V. Tumour Angiogenesis and Angiogenic Inhibitors: A Review. J Clin Diagn Res 2015; 9: XE01-XE05.

[3] Hsu KS, Guan BJ, Cheng X, Guan D, Lam M, Hatzoglou M, Kao HY. Translational control of PML contributes to TNFα-induced apoptosis of MCF7 breast cancer cells and decreased angiogenesis in HUVECs. Cell Death Differ 2016; 23: 469-83.

[4] Bertolini F, Marighetti P, Martin-Padura I, Mancuso P, Hu-Lowe DD, Shaked Y, D'Onofrio A. Anti-VEGF and beyond: shaping a new generation of anti-angiogenic therapies for cancer. Drug Discov Today 2011; 16: 1052-60.

[5] Zhao Y, Adjei AA. Targeting Angiogenesis in Cancer Therapy: Moving Beyond Vascular Endothelial Growth Factor. Oncologist 2015; 20: 660-73.

[6] Gacche RN, Meshram RJ. Targeting tumor micro-environment for design and development of novel anti-angiogenic agents arresting tumor growth. Prog Biophys Mol Biol 2013; 113: 333-54.

[7] Kwon OS, Jeong MS, Kim B, Kim SH. Antiangiogenic Effect of Ethanol Extract of Vigna angularis via Inhibition of Phosphorylation of VEGFR2, Erk, and Akt. Evid Based Complement Alternat Med 2015; 2015: 371368.

[8] Luo JC, Peng YL, Chen TS, Huo TI, Hou MC, Huang HC, Lin HC, Lee FY. Clopidogrel inhibits angiogenesis of gastric ulcer healing via downregulation of vascular endothelial growth factor receptor 2. J Formos Med Assoc 2015; S0929-6646: 00278-8.

[9] Wang Y, Li JX, Wang YQ, Miao ZH. Tanshinone I inhibits tumor angiogenesis by reducing Stat3 phosphorylation at Tyr705 and hypoxia-induced HIF-1α accumulation in both endothelial and tumor cells. Oncotarget 2015; 6: 16031-42.

[10] Hyman DM, Puzanov I, Subbiah V, Faris JE, Chau I, Blay JY, Wolf J, Raje NS, Diamond EL, Hollebecque A, Gervais R, Elez-Fernandez ME, Italiano A, Hofheinz RD, Hidalgo M, Chan E, Schuler M, Lasserre SF, Makrutzki M, Sirzen F, Veronese ML, Tabernero J, Baselga J. Vemurafenib in Multiple Nonmelanoma Cancers with BRAF V600 Mutations. N Engl J Med 2015; 373: 726-36.

[11] Yang Y, Cong H, Han C, Yue L, Dong H, Liu J. 12-Deoxyphorbol 13-palmitate inhibits the expression of VEGF and HIF-1α in MCF-7 cells by blocking the PI3K/Akt/mTOR signaling pathway. Oncol Rep 2015; 34: 1755-60.

[12] Beazley-Long N, Gaston K, Harper SJ, Orlando A, Bates DO. Novel mechanisms of resistance to vemurafenib in melanoma - V600E B-Raf reversion and switching VEGF-A splice isoform expression. Am J Cancer Res 2014; 5: 433-41.

[13] Zhou Z, Zhao C, Wang L, Cao X, Li J, Huang R, Lao Q, Yu H, Li Y, Du H, Qu L, Shou C. A VEGFR1 antagonistic peptide inhibits tumor growth and metastasis through VEGFR1-PI3K-AKT signaling pathway inhibition. Am J Cancer Res 2015; 5: 3149-61.

[14] Aoki M, Batista O, Bellacosa A, Tsichlis P, Vogt PK. The akt kinase: molecular determinants of oncogenicity. Proc Natl Acad Sci U S A 1998; 95: 14950-5.

[15] Liu Y, Ling Y, Qi Q, Zhu M, Wan M, Zhang Y, Zhang C. Trastuzumab increases the sensitivity of HER2-amplified human gastric cancer cells to oxaliplatin and cisplatin by affecting the expression of telomere-associated proteins. Oncol Lett 2015; 9: 999-1005.

[16] Chi BJ, Du CL, Fu YF, Zhang YN, Wang RW. Silencing of CCR7 inhibits the growth, invasion

and migration of prostate cancer cells induced by VEGFC. Int J Clin Exp Pathol 2015; 8: 12533-40.

[17] Chang HN, Huang ST, Yeh YC, Wang HS, Wang TH, Wu YH, Pang JS. Indigo naturalis and its component tryptanthrin exert anti-angiogenic effect by arresting cell cycle and inhibiting Akt and FAK Signaling in Human vascular endothelial cells. J Ethnopharmacol 2015; S0378-8741: 30117-3.

[18] Lee SH, Jung YD, Choi YS, Lee YM. Targeting of RUNX3 by miR-130a and miR-495 cooperatively increases cell proliferation and tumor angiogenesis in gastric cancer cells. Oncotarget 2015; 6: 33269-78.

[19] Fu Q, Kim S, Soto D, De Arcangelis V, DiPilato L, Liu S, Xu B, Shi Q, Zhang J, Xiang YK. A long lasting β1 adrenergic receptor stimulation of cAMP/protein kinase A (PKA) signal in cardiac myocytes. J Biol Chem 2014; 289: 14771-81.

[20] Li C, Yang D, Zhao Y, Qiu Y, Cao X, Yu Y, Guo H, Gu X, Yin X. Inhibitory Effects of Isorhamnetin on the Invasion of Human Breast Carcinoma Cells by Downregulating the Expression and Activity of Matrix Metalloproteinase-2/9. Nutr Cancer 2015; 11: 1-10.

[21] Awada G, Kourie HR, Awada AH. Novel mechanisms and approaches in the medical therapy of solid cancers. Discov Med 2015; 20: 33-41.

[22] Fan M, Zhang J, Wang Z, Wang B, Zhang Q, Zheng C, Li T, Ni C, Wu Z, Shao Z, Hu X. Phosphorylated VEGFR2 and hypertension: potential biomarkers to indicate VEGF-dependency of advanced breast cancer in anti-angiogenic therapy. Breast Cancer Res Treat 2014; 143: 141-51.

[23] Yang GW, Jiang JS, Lu WQ. Ferulic Acid Exerts Anti-Angiogenic and Anti-Tumor Activity by Targeting Fibroblast Growth Factor Receptor 1-Mediated Angiogenesis. Int J Mol Sci 2015; 16: 24011-24031.

[24] Qu W, Wang Y, Wu Q, Liu J, Hao D. Emodin inhibits HMGB1-induced tumor angiogenesis in human osteosarcoma by regulating SIRT1. Int J Clin Exp Med 2015; 8: 15054-64.

Supplementary materials

Lactate dehydrogenase (LDH) toxicity assay

The LDH released into cell cultures is an index of cytotoxicity and evaluation of the permeability of cell membrane. HUVEC were seeded in 96-well plate at a density of 2×10^5 cells per well. After incubation with vehicle (0.1% DMSO), 1% Triton X-100 or various concentrations of vemurafenib for 24 h, cell supernatants were collected and analyzed for LDH activity using LDH cyto-toxicity assay kit from Keygen biotech [1]. The absorbance of formed formazan was read at 490 nm on a microplate reader.

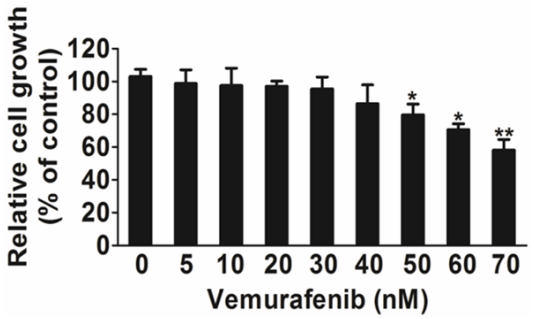

Figure S1. HUVEC cells were exposed to indicated concentrations of vemurafenib for 24 h. Cell viability was determined by One solution cell proliferation assay. The data are presented as mean ± SD. The values are expressed as percentage of viable cells normalized to percentage of viable cells in 0.1% DMSO-treated cells.

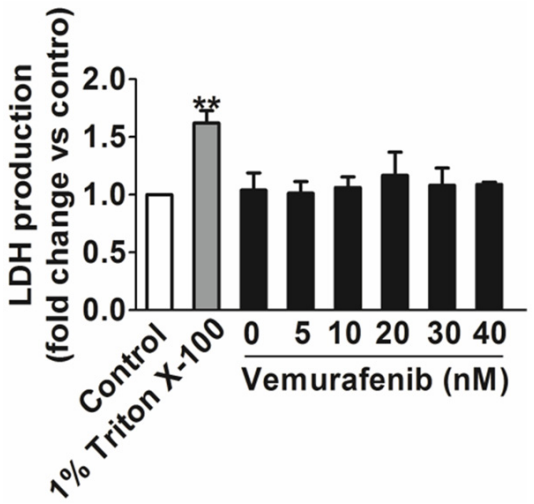

Figure S2. Vemurafenib administration did not result in LDH release, indicating vemurafenib brought little toxic effects on HUVEC (data are presented as means ± SD, n = 6, $**P < 0.01$ versus control).

Reference

[1] Kakanj M, Ghazi-Khansari M, Zare Mirakabadi A, Daraei B, Vatanpour H. Cytotoxic Effect of Iranian Vipera lebetina Snake Venom on HUVEC Cells. Iran J Pharm Res 2015; 14: 109-114.